Rock and Soil Mechanics

Volume 43 | Issue 8 Article 3

9-30-2022

Multi-scale analysis of damage evolution of freezing-thawing red sandstones

Hui-mei ZHANG

Yun-fei WANG

Rock and Soil Mechanics 2022 43(8): 2103−2114 ISSN 1000−7598
https: //doi.org/10.16285/j.rsm.2021.6726 rocksoilmech.researchcommons.org/journal

Multi-scale analysis of damage evolution of freezing-thawing red sandstones

ZHANG Hui-mei, WANG Yun-fei

Department of Mechanics, Xi'an University of Science and Technology, Xi'an, Shaanxi 710054, China

Abstract: We take red sandstone as the research object and apply the freeze-thaw cycles, CT scans and mechanical properties experiments. We use image processing technology combined with genetic algorithm optimization model to achieve the denoise, enhancement, segmentation and three-dimensional reconstruction of CT scan images after 0, 5, 10, 20, and 40 freeze-thaw cycles. With the damage identification and comparative study of the same object across scales, we established a prediction formula of elastic modulus deterioration based on mesoscopic damage. Therefore, the macroscopic mechanical behavior of freeze-thaw red sandstones can be interpreted from the physical nature of the material meso-structure. The results show that genetic algorithm based on image maximum entropy can quickly and accurately select the threshold for image segmentation, and achieve the recognition of matrix and defects in rock meso-structure. With the increase of freezing and thawing cycles, the porosity of rock increases, and the fractal dimension of pore decreases. On the meso-scale, the evolution shows that the pores expand and the number increases, but the structural complexity decreases. The macroscopic and mesoscopic damage variables defined by the traditional methods are based on the effective bearing area and elastic modulus, and they fail to fully consider the damage physical mechanism and the internal structure information of the material. The damage evolution curves are different. Based on the two physical mechanisms, we define the meso-damage variable and the macro-damage variable that considers the natural rock damage, which achieves the combination of macroscopic and mesoscopic damages. Finally, according to the relationship between meso-structure evolution and macroscopic mechanical response in the process of freeze-thaw cycles, we propose a prediction formula of elastic modulus degradation, and analyze the different dominant roles of pore size and pore structure morphology through the damage process. We interpret the mechanical mechanism of macroscopic sandstone freeze-thaw damage based on the meso-structure physical mechanisms.

Keywords: freeze-thaw sandstone; damage; multi-scale; physical mechanism; macro-meso combination

1 Introduction

The China 14th Five-Year Plan proposes the construction projects as a country powerful in transportation. Among them, the maintenance and construction of border passages, land bridge corridors, and national water network backbone projects are mostly located in perennial and seasonally frozen regions. These can be sensitive to climate change, and freeze-thaw engineering disasters can occur frequently. The effect of freeze-thaw cycles in cold regions on rocks is essentially the uneven shrinkage and expansion of rock minerals and the phase transition of water and ice, which lead to the continuous expansion of micro-defects, the intensification of damage, and the deterioration of macroscopic mechanical properties[1−2]. The deformation and failure of rock is a continuous damage process caused by the accumulation and expansion of its internal defects. The damage accumulation of meso-structure is the key to induce the failure of macroscopic phenomenological rock structure. Therefore, it is an important development to establish the macro-mesoscopic multi-scale identification and mechanism evaluation of the freeze-thaw-induced rock damage, which helps understand the problem of rock freeze-thaw damage comprehensively. It is important both for the theory and for the engineering application in order to prevent and control the engineering freezing disasters in cold regions.

Rock damage has a significant scale effect. The meso-scale structure has the characteristics of orderly distribution, which is not straightforward to conduct an intuitive study. The damage evolution is a typical black-box problem, and it has always been difficult issue that hinders the in-depth understanding of the physical nature of the rock mass deformation and failure. In recent years, CT scanning technology has received extensive attention as a non-destructive testing method. Yang et al.[3] first use the non-destructive CT testing technology to detect the damage of the pore structure of frozen-thawed rock. They show the relation between the CT number distribution and the rock damage variable, and present the qualitative and quantitative research on the rock damage at the mesoscopic level. Appoloni et al.[4] study the relations between the size and distribution of CT numbers and the rock damage under different loads. They provide a method for predicting rock physical properties based on meso-parameters. Zhu et al.[5] use CT scanning to obtain the density distribution and statistical characteristics inside the rock material during uniaxial compression failure, which can be used to identify the activity of micro-cracks. Ma et al. [6] carried out CT scanning tests of shale samples at different hydration stages. They propose that the sharp increase of the shale damage can be identified by the change in the gray-scale histogram of the CT image from a unimodal to a

Received: 14 October 2021 Revised: 12 February 2022
This work was supported by the National Natural Science Foundation of China (12172280, 42077274, 41907259) and the Key Program of Natural Science Foundation of Shaanxi (2020JZ-53).
First author: ZHANG Hui-mei, female, born in 1968, PhD, Professor, PhD supervisor, mainly engaged in the teaching and research work of theoretical analysis and engineering application of rock freeze-thaw damage in cold regions. E-mail：zhanghuimei68@163.com

bimodal. With the progress made in studying the CT images and rock damage, some work start to show the effort on further processing of CT images. To improve the image visualization, Han et al.[7] use the density segmentation enhancement technique to correlate the CT value with the material density, and obtain the crack propagation variation of concrete specimens under different strain rates. Liu et al.[8] use the ternary segmentation technology to process frozen rock CT images. They identify and quantitatively express the contents of the three-phase media including water, ice and rock, and they discuss the influence of meso-parameters on the damage characteristics of frozen rock. Zhang et al.[9] use the *K*-means clustering algorithm to identify two-dimensional pores in CT scanned images, and they quantitatively describe the freeze-thaw damage of rocks based on the concept of effective bearing zone reduction. These computer-based image processing methods are effective, and they provide the foundation for the in-depth study of the mesoscopic structure of rocks.

Nowadays, the popular yet difficult point in rock damage mechanic study is to quantitatively analyze the micro- and meso-structure in the rock and to connect these with the macroscopic properties of the material [10]. Peng et al. [11] use grayscale CT images to reflect the fractal characteristics of rock pore structure. Based on this, they find that given the same porosity, the larger the internal pore fractal dimension, the more complex the pore structure. Li et al. [12] calculate the fractal dimension of rocks under different loading conditions by using the box-counting dimension method. They find that the failure process of rock samples does have fractal characteristics, and the fractal dimension can quantitatively characterize the failure process of rock samples. Park et al.[13] use CT scanning technology to study the damage of pore structure and the expansion of internal micro-cracks in igneous rocks under the action of freeze-thaw cycles. De Kock et al.[14] analyze the expansion process of limestone mesoscopic fractures under the actions of both the capillary water absorption and the freezing-thawing cycles. Chen et al.[15] carry out CT scanning experiments on shotcrete, and study the variation of micropores inside the concrete with the iteration of freeze-thaw cycles. Liu et al.[16] build a three-dimensional digital core model using micro-CT technology to characterize the pore structures of sandstone reservoir rocks. Song et al.[17] carry out uniaxial-loading, real-time CT scanning on the sandstones at different temperatures. They quantitatively study the damage evolution of frozen rock based on the proportional relationship between the CT number *H* value and the density. Lang et al. [18] reconstruct a mesoscopic model based on CT scan images. They use numerical simulation of the three-dimensional Brazilian splitting test to study the effect of spatial pore distribution on its macroscopic mechanical properties.

The studies listed above show that the damage description based on the meso-reference quantity is important for understanding the crack propagation and the failure process of rock mass. However, there are still difficulties in the quantitative relationship between the evolution of the meso-structure and the macroscopic mechanical response. At the same time, there are mainly the following problems listed below when considering the mathematical description of how the mesoscopic structure of the material can be related to the damage, and when considering the reasonable characterization of the development of mesoscopic damage with many parameters and complex structures. (1) There is no panacean segmentation theory in image processing. Extracting the meso-structure image of the material and converting it into the mesoscopic damage development representation have the limitations including the instrument accuracy and image processing difficulties. (2) How to select the appropriate mathematical expressions to accurately quantify the meso-structure information of rock materials. (3) It is not straightforward to introduce the mesoscopic mechanism into the macroscopic variables through proper mathematical description, and not straightforward to establish the relations to the macroscopic mechanical properties. Therefore, if possible, the damage identification of the same object across meso- and macro-scales is not only helpful for understanding the rock damage mechanism, but also provides important information for the development of multi-scale damage models.

In order to seek the essential characteristics of rocks, this study aims at freeze-thaw damage characterization, which is based on the freeze-thaw environment with focuses on the rock meso-structure and the corresponding macroscopic properties. It is a multi-scale study on the rock freeze-thaw damage identification. We take the red sandstone as the research object and apply freeze-thaw cycles, CT scans and mechanical property tests. We use digital image processing technology to extract rock mesoscopic features and perform 3D reconstruction for visualization. We fully consider the pore size and structural morphological changes of sandstone, and quantitatively characterize the meso-damage. We consider the initial damage and the sandstone strength to quantitatively characterize the macroscopic damage. We establish the relationship between the macroscopic and the mesoscopic damage evolution, and provide a new method for characterizing rock freeze-thaw damage on multiple scales.

2 Freeze-thaw cycle, CT scan and mechanical properties experiments

2.1 Experiment design

We select the Cretaceous sandstone for the experiments, which is widely distributed in the cold region and can be considered representative. The whole process has been completed with computer interactions. The cylindrical rock samples with size of Φ50 mm × 100 mm are prepared by water drilling method according to the international standards. We first manually exclude the specimens with obvious defects in appearance, and then use a non-metallic

acoustic wave detector to select 16 specimens with similar P-wave velocities. We saturate the test pieces with water. Table 1 lists the basic physical parameters of the red sandstone samples measured by the drainage method.

Table 1 Basic physical parameters of red sandstone samples

Porosity /%	Dry density /(g • cm^{-3})	Saturated density /(g • cm^{-3})	Saturated wave velocity /(m • s^{-1})
14.31	1.78	2.01	1 450

Fig. 1 Freeze-thaw test process

As shown in Fig.1, the freeze-thaw experiment has been completed using the XMT-605 rapid freeze-thaw machine. The specimens are placed naturally in the equipment without any constraints and are in an open and saturated state. We set the temperature to start from 20 °C to –20 °C, and then return to 20 °C as a freeze-thaw cycle. The cycle duration is controlled by the temperature, and each cycle takes about 6 hours. The maximum number of freeze-thaw cycle is 40. When the number of freeze-thaw cycles reaches 0 (not frozen-thawed yet), 5, 10, 20, and 40 times, we take out the 3 specimens and wipe off the surface moisture. We use the MTS815 electro-hydraulic servo rock testing system to measure the mechanical properties, and therefore obtain the mechanical parameters of red sandstone under different freeze-thaw cycles. In addition, in order to compare the changes of the meso-structure of specimens under the same conditions, we select the same specimen and put it into the Compact-225 industrial CT machine for simultaneous CT scanning under different iterations of freeze-thaw cycles. The scanning sections are numbered layer by layer from top to bottom, for the convenience of describing the overall freeze-thaw damage and the deterioration effect of the rock sample. The image size of each layer is 500 pixels×500 pixels. The actual size corresponding to one pixel is 0.1 mm, as shown in Fig. 2, a schematic diagram of the CT scanning planes.

2.2 Experiment results

Table 2 lists the mechanical parameters including elastic modulus, compressive strength and peak strain of red sandstone under different freeze-thaw cycles obtained by the mechanical property tests.

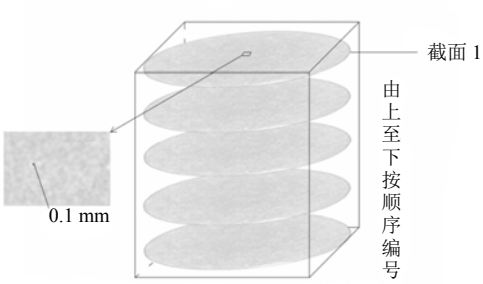

Fig. 2 Diagram of the CT scan plane

Table 2 Mechanical parameters of red sandstone under different freeze-thaw cycles

Number of freeze-thaw cycles n	Elastic modulus E /GPa	Compressive strength σ_c /MPa	Peak strain ε_c /10^{-3}
0(water saturated)	1.160	4.23	4.18
5	0.805	4.02	4.56
10	0.705	3.80	5.20
20	0.408	3.74	5.92
40	0.371	3.30	6.06

With the CT scanning, for each freeze-thaw cycle, about 850 cross-sectional CT-scanned images can be obtained stacked along the height of the rock sample. We take the 500th layer of the scanned raw images as an example, Fig. 3 shows the CT scanned images after 0, 5, 10, 20, and 40 freeze-thaw cycles. Fig. 4 shows a grayscale distribution of the CT scanned images after 10 freeze-thaw cycles.

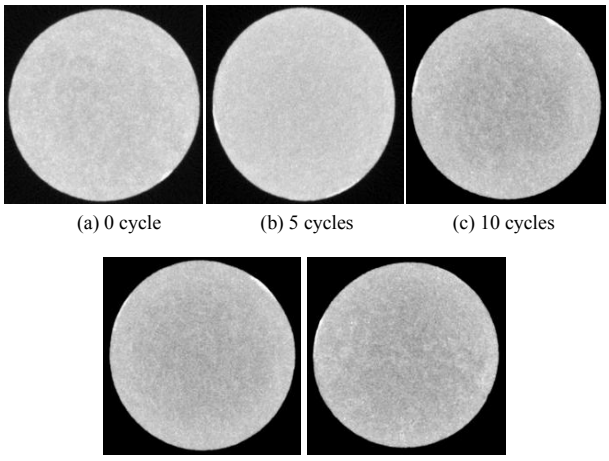

Fig. 3 CT scan images of the same section but with different freeze-thaw cycles

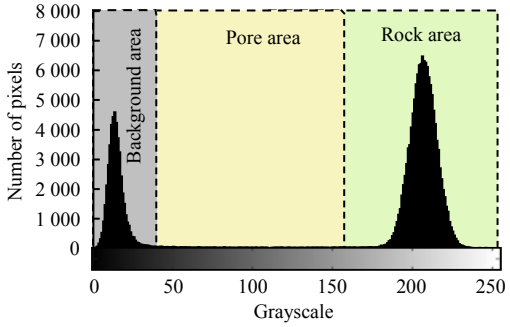

Fig. 4 Gray distribution of CT scanning images

As shown by Figs. 3 and 4, the CT scan image has the grayscale range from 0 to 255, in which the pure black has the grayscale of 0 and the pure white has the grayscale of 255. In the rock area, the grayscale value of the pixel is proportional to the rock particles density at the corresponding position. The peak-to-trough range of the grayscale distribution of the image is wide. The grayscale values of rock particles and defects are both between 50 and 255, which makes it difficult to distinguish and filter out the pores. In addition, due to the limitations of the imaging system and equipment during the scanning process, the acquired images suffer from noise. Noise usually can be observed by the extreme grayscale values in the image and presents pure white or black pixels, which can greatly degrade the image quality. Therefore, digital image processing should be used to preprocess the original image before studying the rock mesoscopic features.

3 CT image preprocessing

The aim of this section is to improve the image visualization, to reduce the noise effects, and to accurately express the rock mesoscopic damage quantitatively. In this paper, we use image processing technology combined with genetic algorithm to optimize the model to achieve the denoising, augmentation and segmentation of CT images.

3.1 Image denoising and augmentation

We use a median filter to denoise the image. We set the neighborhood window to be 3×3 to reduce the noise effects on the image as much as possible while ensuring that the signal is not affected. At the same time, in order to facilitate the subsequent image binarization and to intuitively distinguish between the rock matrix and the pore, we further apply an image augmentation after denoising. We use the histogram equalization and Laplacian sharpening to process the image[19], respectively, and obtain the images with obvious grayscale contrast, as shown in Fig.5.

As shown in Fig.5 that after the histogram equalization, the range of the grayscale distribution has been expanded, and the resolution of rock particles and defects has been increased. However, although the grayscale contrast has been improved, the grayscale distribution and mesoscopic information have been changed to some extent, which results in the image distortion. In contrast, the Laplacian sharpening filtering evaluates the degree of change in image pixels through a second-order differentiation. When the grayscale of the central pixel is lower than the average of its neighbored pixels, its grayscale is reduced; otherwise, it is increased. This method enhances the details of the image without changing the original grayscale distribution and should be better than the histogram equalization method because it ensures the image reality as much as possible. Therefore, in this paper, median filtering and Laplacian sharpening are selected to process all the original CT scanned images, which provides the fundamentals for selecting the thresholds in the subsequent image segmentation process.

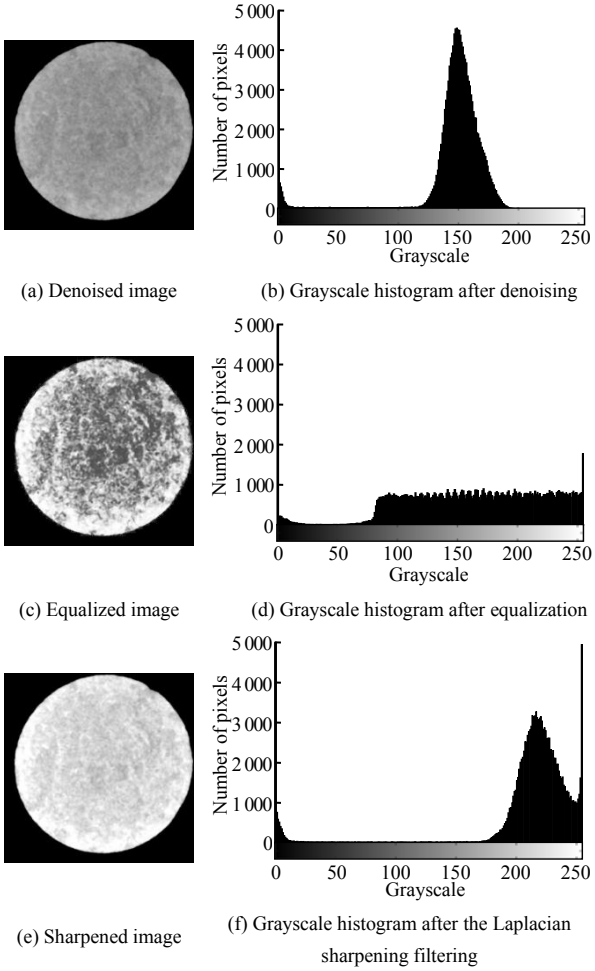

(a) Denoised image (b) Grayscale histogram after denoising

(c) Equalized image (d) Grayscale histogram after equalization

(e) Sharpened image (f) Grayscale histogram after the Laplacian sharpening filtering

Fig. 5 Image denoising, enhancement, and the gray histogram

3.2 Optimization model with genetic algorithm

For image segmentation, the choice of the threshold is important that determines the ratio of the pore area against the rock section. Therefore, the method that finds the optimal threshold is also the key in image binarization. In our study, we first use the traditional bimodal method and the Otsu's thresholding method for processing. However, since the grayscale distribution of rock cross-sections has no obvious bimodal characteristics, the segmentation quality is not ideal. The *K*-means clustering algorithm [20] works by comparing the similarity and difference of data. The result is decent, but it still requires a manual selection of the initial cluster center. The results of using different cluster centers are also different, and therefore are not stable enough.

In this paper, we combine the maximum entropy method and the genetic algorithm. The maximum entropy method calculates the threshold corresponding to the maximum entropy of the image and then segments the image, which can ensure the maximum information between the pore area and the rock area. It is an effective image segmentation method.

The method selects a threshold t (with the grayscale range $0 \leqslant t \leqslant 255$), which can divide the image into two parts: the pore area and the rock area. The calculated cumulative probabilities of the two areas are

$$\left.\begin{aligned} P_{\mathrm{T}}(t) &= \sum_{i=1}^{t} p(i) = p(t) \\ P_{\mathrm{B}}(t) &= \sum_{i=t}^{255-t} p(i) = 1 - p(t) \end{aligned}\right\} \tag{1}$$

where $p(i)$ is the probability of each grayscale value that can occur; $P_{\mathrm{T}}(t)$ is the cumulative probability of grayscale in the pore area; and $P_{\mathrm{B}}(t)$ is the cumulative probability of grayscale in the rock area.

Image entropy can reflect the amount of random information in the image and the complexity of the image. The image entropy $H_{\mathrm{T}}(t)$ and $H_{\mathrm{B}}(t)$, corresponding to the pore and the rock areas, are calculated as

$$\left.\begin{aligned} H_{\mathrm{T}}(t) &= -\sum_{i=1}^{t} \frac{p(i)}{P_{\mathrm{T}}(t)} \lg \frac{p(i)}{P_{\mathrm{T}}(t)} \\ H_{\mathrm{B}}(t) &= -\sum_{i=t}^{255-t} \frac{p(i)}{P_{\mathrm{B}}(t)} \lg \frac{p(i)}{P_{\mathrm{B}}(t)} \end{aligned}\right\} \tag{2}$$

The image entropy $H(t)$ is calculated with different thresholds t. When the image entropy reaches its maximum, the corresponding threshold t should give the best image segmentation result[21].

$$H(t) = H_{\mathrm{T}}(t) + H_{\mathrm{B}}(t) \tag{3}$$

In order to efficiently and accurately solve the threshold corresponding to the maximum entropy, we use a genetic algorithm to exhaustively search all the grayscale values and assign them to the threshold t in Eq. (1). We use Eq. (3) as the fitness function. We decode the chromosome array into values between 0 and 255 to correspond to the possible threshold between 0 and 255. In addition, this paper follows the idea as stated in the literature [8] and notices the requirement that the algorithm needs to search all the grayscale values exhaustively. We consider the computational efficiency, and search for the critical value of the population and the required iteration as long as the solution accuracy can be guaranteed. The algorithm design is a population of 100 and a fixed iteration of 20. The workflow is shown in Fig. 6.

The model combines the maximum entropy method and the genetic algorithm to search for the optimal threshold for each image based on probability. It avoids the errors caused by the manual selection of thresholds. In addition, the algorithm can adaptively adjust the search direction. The computational speed is fast. The ability to find the optimal value is excellent. The obtained results are good.

3.3 Image binarization

Based on the digital image and matrix theory, we apply a binary transformation to process the original grayscale image matrix as

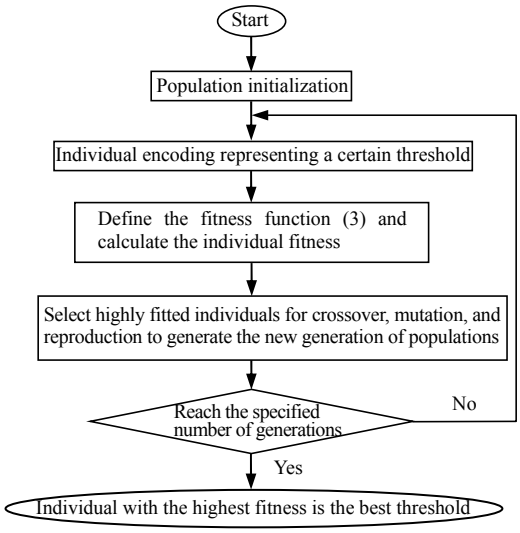

Fig. 6 Algorithm workflow

$$f(x,y) = \begin{cases} 0 & T < t \\ 1 & T \geqslant t \end{cases} \tag{4}$$

where $f(x,y)$ gives the value at the corresponding matrix position; T is the grayscale value of the pixel at that position; and t is the optimal threshold solved by the genetic optimization model.

A matrix consisting of zeros and ones can be obtained after the processing using Eq.(4). The matrix presents a binarized image with sharp contrast showing black against white. A matrix element 0 is black, indicating the pores and low-density rock particles that have lost their original bearing capacity due to damage. A matrix element 1 is white, which represents the rock particles with bearing capacity. After the processing, the binarized image of rock section number 500 is obtained as shown in Fig. 7.

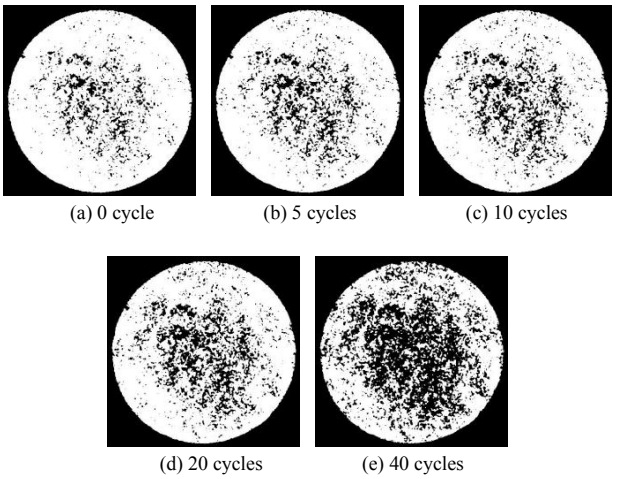

Fig. 7 Binary images of the same section but with different freeze-thaw cycles

As illustrated by Fig.7, the black pixels representing pores in the binarized image gradually increase with the increase of the freeze-thaw cycles, indicating that the accumulation of freeze-thaw damage increases.

Freeze-thaw effect promotes the secondary expansion of primary defects, and the damage to the central part is more obvious which contains more primary pores.

4 Rock meso-feature extraction

To quantitatively characterize the evolution of rock meso-structure during freezing and thawing, it is necessary to extract mesoscopic features from the preprocessed CT images, so as to further study the nature of rock damage.

4.1 Porosity of rock sections

Based on the digital image and matrix theory, we calculate the ratio of element 0 in the cross-sectional binary image matrix with respect to all the matrix elements. We exclude the background area and obtain the porosity of the rock section. Since the top and bottom CT scan images are incomplete, the corresponding data are not valid. Therefore, in this paper, we select images with section numbers between 50 and 750 for the porosity estimation. The data image is dense and highly discrete, resulting in a densely sampled cross-sectional porosity plot. To avoid that, this paper uses a step size of 20 to equally sample the images to plot the porosity, which should make it easier to observe the pore distribution variation along the cross-sectional direction. We plot the cross-sectional pore distribution in Fig. 8, in which the small one is the porosity distribution of rock sections numbered from 600 to 700 after applying 40 freeze-thaw cycles.

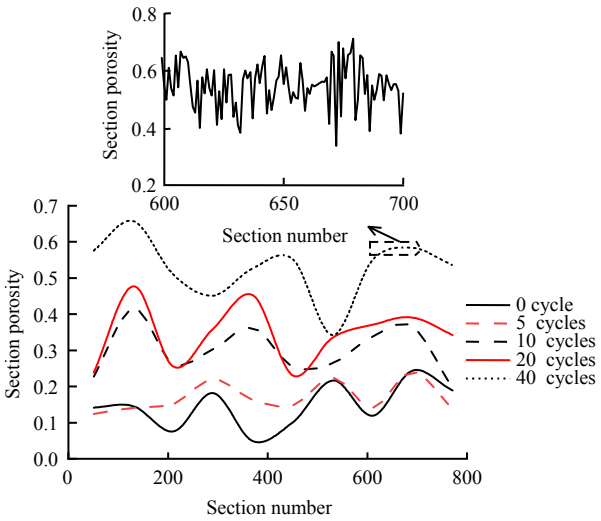

Fig. 8 Porosity distribution of the rock section under different freeze-thaw cycles

As shown in Fig.8, with the continuous increase of freeze-thaw cycles, the porosity of the rock section increases in general. The porosity distributions both show the disorder considering the different sections of the same specimen and considering the same section but with different freeze-thaw cycles. This indicates that rock materials have complex multi-scale structural characteristics and spatial randomness. And due to the large number of scanned layers, there is the positioning deviation of the same numbered section under different freeze-thaw cycles. In addition, the analysis of CT scan images is essentially two-dimensional, and it can only obtain the pore distribution on the cross sections. It is still difficult to describe the overall mesoscopic structure. Therefore, there are certainly errors to some extent in the quantitative analysis of rock freeze-thaw damage if we only use cross-sectional porosity.

4.2 3D reconstruction visualization and the volume porosity

The aim is to better describe the spatial distribution characteristics and the evolution of the overall pore structure in the sandstone during the freeze-thaw process, as well as to quantitatively describe the meso-damage and the deterioration of the sandstone. In this paper, the binarized images are used for 3D reconstruction and visualization, and the 2D slice data are processed into 3D volume data. A three-dimensional pore model is established that can characterize the internal pore structure of the red sandstone clearly and intuitively, as plotted in Fig.9, where the blue color in the figure denotes the pore structure. As shown by the three-dimensional pore structure model in the figure, the internal pore structure of the rock has changed significantly before the macroscopic damage occurs. As the number of freeze-thaw cycles increases, the porosity increases accordingly. Under the action of 0 freeze-thaw cycle, the pore diameters of the pores are small and distributed independently. In contrast, when the freeze-thaw cycles reach 40 times, some pores are connected to each other, and the distribution is dominated by connected pores.

In order to accurately quantify the development of the overall pore structure of the rock and study the damage and deterioration of the rock meso-scale, our study estimates the volume ratio of the porous structure of the rock, and obtains the porosities of the rock mass under different freeze-thaw cycles as listed in Table 3.

In Table 3, the porosity of the specimen under 0 freeze-thaw cycle is about 14.31%, which is consistent with the porosity measured by the drainage method. This shows that the segmentation and the quantification data are true and reliable.

4.3 Fractal dimension of pore structure

As shown by the 3D reconstruction model, the pore structure and the morphology inside the rock are extremely complex. In this study, a certain section is selected for the two-dimensional image visualization. The vertical axis shows the grayscale value, and the three-dimensional model of the mesostructure of the rock section is generated as shown in Fig. 10.

As shown by Fig.10, pores with different depths are connected to each other, which present different spatial distribution patterns. Therefore, the study only considering the variation of porosity cannot accurately describe the geometrical nature of the randomly distributed pores of the frozen-thawed rocks. We have to consider the morphological changes in the pore structure. Since the 21st century, the use of fractal

geometry[22–24] has provided an effective method to quantitatively describe the complexity of pore structures. The internal damage evolution of rocks has fractal characteristics and effects. Thus, the fractal dimension of the pore structure (referred as the pore fractal dimension below) can effectively describe the characteristics of the pore structure inside the rock as well as reflecting its damage degree.

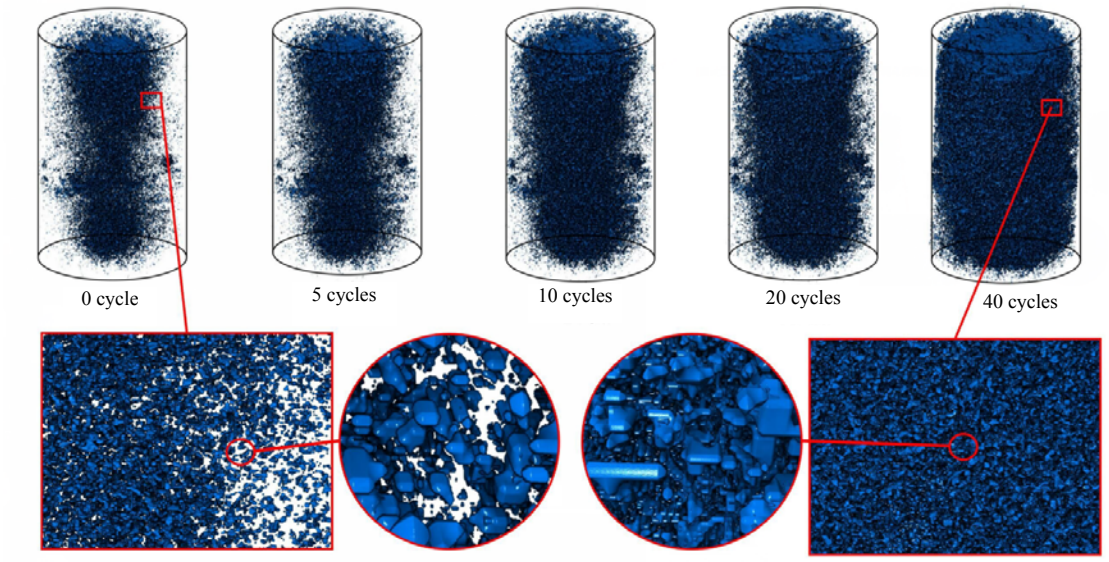

Fig. 9 Three-dimensional pore structure models under different freeze-thaw cycles

Table 3 Rock porosity under different freeze-thaw cycles

Number of freeze-thaw cycles n	Volume porosity λ_n /%	Number of freeze-thaw cycles n	Volume porosity λ_n /%
0	14.316	20	32.157
5	15.192	40	54.497
10	31.957		

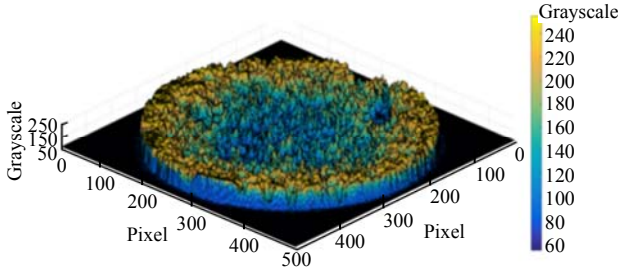

Fig.10 Stereoscopic diagram of the rock cross-section microstructure

In this study, we use the box counting method[24] to calculate the pore fractal dimension of the image. Taking Fig.10 as an example, we use a square with length $\in$ to divide the image into regular grids, and count the number of pores in the grid as $N(\in)$. By changing the length of the square, a set of numbers $N(\in_n)$ can be obtained. We plot the data in the logarithmic scale, and determine the relationship of $\ln N(\in) - \ln \in$ as shown in Fig.11. The fractal dimension B is calculated as

$$B = -\lim \frac{\ln N(\in)}{\ln \in} \tag{5}$$

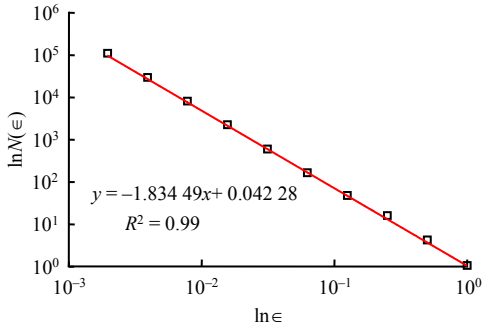

Fig. 11 The linear model fitted in double-logarithmic scales

We calculate the mean value of the pore fractal dimension of the rock section, and obtain the pore fractal dimension under different freeze-thaw cycles, as shown in Table 4.

Table 4 Fractal dimension of rock pores under different freeze-thaw cycles

Number of freeze-thaw cycles n	Pore fractal dimension B_n	Number of freeze-thaw cycles n	Pore fractal dimension B_n
0	1.856 0	20	1.804 8
5	1.843 1	40	1.384 3
10	1.811 5		

The variations of rock porosity and pore fractal dimension are plotted with the number of freeze-thaw cycles, as shown in Fig. 12.

As shown by Fig.12, with the increase of the freeze-thaw cycles, the porosity of sandstone increases continuously, and the pore fractal dimension decreases accordingly. That is, the number and size of pores in the sandstone increase, but the complexity and

self-similarity of the pore structure decrease. The two mesoscopic parameters effectively quantify the size and the degree of morphological change of the pore structure. Combining with the three-dimensional pore structure model under different freeze-thaw cycles shown in Fig.9, it can be seen that under the freeze-thaw action, the primary pores in the rock continue to expand, the size increases and the pores connect with each other. At the same time, the material bonding has been weakened and secondary pores start to appear. The originally complex and disorderly distributed micro-pore structure has evolved into a multi-scale pore structure, in which large defects are dominant, and secondary small pores are developed and dispersed.

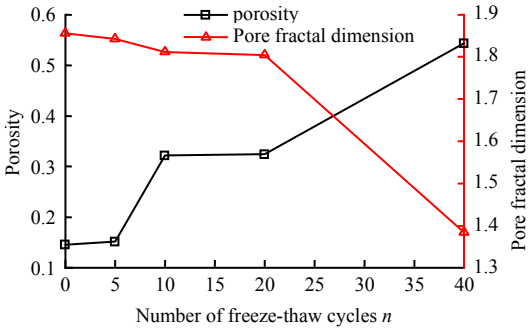

Fig. 12 Variations of porosity and fractal dimension of rock under different freeze-thaw cycles

5 Freeze-thaw damage evolution of the red sandstone

Macroscopic damage mechanics addresses that damage is distributed continuously at the macro-level, and the rock damage characteristics are extracted based on the phenomenon of macro-damage variables. However, it does not consider the physical nature of material deformation and failure. Mesoscopic damage mechanics studies the shape, distribution and evolution characteristics of various damages based on the level of meso-structures such as particles and micro-cracks in the material. Our study selects different metrics and damage benchmarks at two different scales. By using the damage identification and the comparison of the same object across scales, we propose a method to define the damage variable that comprehensively considers the mesoscopic structural information, and explores the relationships between the mesoscopic information and the macroscopic mechanical response of the material.

5.1 Conventional definitions of macro-mesoscopic freeze-thaw damage variables

According to the Kachanov damage theory, the main mechanism of material deterioration is the reduction of effective bearing area due to micro-defects[25]. Among the mesoscopic features extracted in this paper, the porosity of the rock body is the ratio of the failure volume inside the rock to the theoretical rock bearing volume. Therefore, the mesoscopic freeze-thaw damage variable defined by the conventional method can be expressed as

$$D_{\mathrm{n}} = \frac{\tilde{A}}{A} \tag{6}$$

where A is the theoretical rock bearing volume; $\tilde{A}$ is the failure volume inside the rock.

According to the macroscopic phenomenology, the macroscopic performance of the damage is the deterioration of material mechanical properties, and the degree of deterioration can be characterized by the response of macroscopic mechanical properties. The traditional macroscopic damage variable can generally be expressed by the macroscopic elastic modulus:

$$D'_{\mathrm{n}} = 1 - \frac{E_n}{E_0} \tag{7}$$

where E_0 is the elastic modulus of water saturated sandstone without freeze-thaw action; E_n is the sandstone elastic modulus after different freeze-thaw cycles.

According to Eqs. (6) and (7) and the data in Tables 2 and 3, the conventional macro- and meso-damage evolution are plotted in Fig. 13 showing the variation with different freeze-thaw cycles.

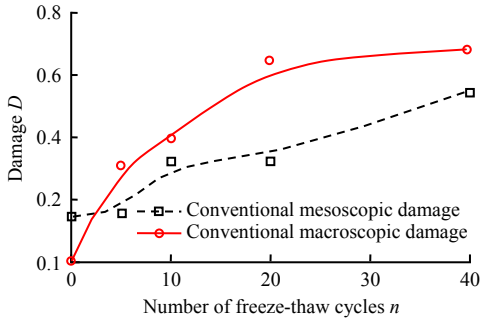

Fig. 13 Macro and meso freeze-thaw damage evolution plots defined by traditional methods

As shown by Fig.13, the macro- and meso-damage of freeze-thaw rocks increase with the increase of freeze-thaw cycles, but the increase paths are quite different. The initial macro-damage variable defined by the traditional method is 0, and the natural damage of the rock has not been considered. The meso-damage and its variation rate are both small. This is consistent with the point discussed in [26], which states that "the absolute change of the porosity of the rock mass is small after multiple freeze-thaw cycles, and an amplification factor needs to be added to match the range of the damage."

In addition, the study [27] introduces a new parameter k to correct the damage range established based on porosity. k is obtained by fitting and has no clear physical meaning. And k is greater than 1, which essentially just amplifies the damage based on porosity, and matches the porosity change to the calculation result of the freeze-thaw damage model.

5.2 Correction of the conventional freeze-thaw damage variable

Research shows that the deterioration of the rock

physical and mechanical properties is the combined result of the reduction of the effective bearing area and the change of the pore structure. The definition of damage variable must consider both two physical mechanisms under the freeze-thaw action. Porosity shows the impact of the effective bearing area reduction on the freeze-thaw damage, whereas pore fractal dimension can measure the change of the pore structure. Pore fractal dimension is positively correlated with the damage of frozen-thawed rock. The larger the value, the more complex the pore structure and the more obvious the stress concentration during the freeze-thaw process, and the more serious the damage. In addition, the pore fractal dimension is greater than 1. Consider a correction formula that is based on the product of the pore fractal dimension and the meso-damage variables defined by porosity. The correction not only reflects the positive correlation between the pore fractal dimension and the damage of frozen-thawed rocks, but also responds to the expectation in studies [26–27] on the amplification factor of the absolute change of the porosity. At the same time, it considers another physical mechanism of damage, which gives the explicit physical meaning to the parameter k in literature [27].

Therefore, our study defines the mesoscopic freeze-thaw damage variable based on porosity and pore fractal dimension, and obtains the corrected mesoscopic damage variable of frozen-thawed rock as

$$D_{\mathrm{B}n}=D_{\mathrm{n}}B_n=\left(\frac{\tilde{A}}{A}\right)_n\left[-\lim\frac{\ln N(\in)}{\ln\in}\right]_n \tag{8}$$

where $D_{\mathrm{B}n}$ is the corrected mesocopic rock damage variable; B_n is the pore fractal dimension of the rock under different freeze-thaw cycles.

Conventional macroscopic freeze-thaw damage variable is defined based on the elastic modulus of water-saturated rocks without any freeze-thaw action. However, it does not consider the natural damage of the rock, resulting in an initial damage value of 0. Therefore, in order to accurately define the macroscopic damage variable of frozen-thawed rock, the elastic modulus E of the undamaged rock needs to be determined. Nevertheless, there are no undamaged rocks in nature, and E cannot be directly measured by experiments. In this paper, we use the damage properties of water-saturated rocks without any freeze-thaw action to derive inversely the undamaged elastic modulus. We introduce the freeze-thaw meso-damage variable into the calculation of rock elastic modulus to reduce the effect of natural damage, and obtain the undamaged elastic modulus as

$$E=\frac{E_0}{1-B_0\lambda_0} \tag{9}$$

where λ_0, B_0 and E_0 are the volume porosity, pore fractal dimension and elastic modulus of the red sandstone without any freeze-thaw cycles, respectively.

Based on the undamaged elastic modulus correction, the macroscopic damage variable of frozen-thawed rock can be expressed as

$$D_{\mathrm{E}n}=1-\frac{E_n}{E} \tag{10}$$

According to Eq. (9), the undamaged elastic modulus E is solved as 1.57 GPa. Substituting it into Eq. (10), the real macroscopic damage variable can be solved.

Fig. 14 plots the corrected macro and mesoscopic freeze-thaw damage variations.

As shown by Fig.14, the mesoscopic damage variable defined based on the two physical mechanisms including pore size and structures presents good agreement with the macroscopic damage variable defined by considering the natural damage of the rock. This achieves the damage identification that covers different scales for the same object. It combines the material mechanical behaviour inside the rock with the rock macroscopic mechanical behaviour. It quantitatively describes the relationship between the mesostructure changes and the macroscopic mechanical response during the freeze-thaw cycles.

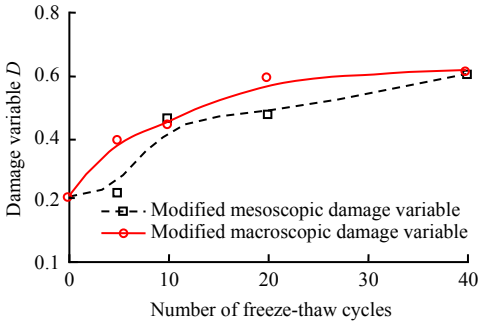

Fig.14 Modified macroscopic and mesoscopic damage evolution plots

5.3 Elastic modulus deterioration prediction based on the meso-damage

In order to understand the effect of the meso-scale freeze-thaw rocks on their macro-scale behaviour and performance, we need to further study the relationship between the rock elastic modulus deterioration and the meso-scale damage variable under the freeze-thaw actions.

Based on the mesoscopic characteristics, the established macroscopic and mesoscopic damage variations are consistent. We fully consider the uncertainty of the characteristics of the frozen-thawed rock meso-structure. By combining Eqs. (8) and (10), we obtain the following relationship between the meso-damage and the elastic modulus as

$$E_n^*=(1-D_{\mathrm{B}n})E \tag{11}$$

where E_n^* is the predicted elastic modulus.

The aim is to obtain an equation to predict the elastic modulus deterioration in a simple form which can be meaningful for practical calculation. We use

Eq. (8) to calculate the rock meso-damage variable under different freeze-thaw cycles. Based on the characteristics of the function, we use an exponential form $D_{Bn}(n)=a-b\times c^n$ to describe the nonlinear characteristics of the meso-damage. The material parameters a and b can represent the damage degree of the rock during a single freeze-thaw cycle. The parameter c represents the nonlinear degree of the rock freeze-thaw damage. Figure 15 shows the resultant of meso-damage variation versus the number of freeze-thaw cycles.

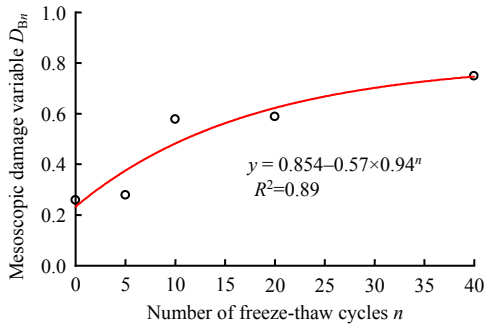

Fig. 15 Relationship between meso-damage variables and freeze-thaw cycles

Substituting the meso-damage variable function shown in Fig.15 into Eq. (11), we obtain the prediction formula of the elastic modulus deterioration based on meso-damage as

$$E_n^*=(0.146+0.57\times0.94^n)E \quad (12)$$

By using Eq.(12), we can quickly predict the elastic modulus of frozen-thawed rocks, and compare the predicted values with the experiment data as shown in Table 5.

Table 5 Comparison of the measured and the predicted elastic modulus

Number of freeze-thaw cycles	Measured elastic modulus /GPa	Predicted elastic modulus /GPa	Error /%
0	1.160	1.120	0.3
5	0.805	0.883	9.7
10	0.705	0.709	0.6
20	0.408	0.488	19.6
40	0.371	0.305	17.8

The analysis of data given in Table 5 shows that the predicted values are in good agreement with the measured values, and therefore the predicted result can show the deterioration trend of the elastic modulus. The error of the predicted elastic modulus reaches 19.6% when the freeze-thaw cycles are 20 times. However, the error does not increase with the increase of freeze-thaw cycles, which can be regarded as an individual case. This proves that the method is feasible to predict the elastic modulus deterioration of the frozen-thawed rocks based on the meso-damage. The model quantitatively depicts the relationship between the meso-structure features and the rock mechanical parameters, which provides an important condition to realize the establishment of multi-scale damage models. The model combines the behaviour of the internal components of the rock with its macroscopic mechanical behaviour. It also provides the theoretical basis for the future mechanical property tests by using the numerical models, which demonstrates its important practical usefulness.

5.4 Analysis of sandstone damage deterioration under the freeze-thaw action

During the freeze-thaw cycles, rocks have experienced the facts including the particle displacement and deformation, the growth of original pores and the development of new pores, the migration and dissipation of water, and the change of local density[28–32]. Based on the above image-based and data-based results, the authors believe that the meso-deterioration of sandstone under freeze-thaw actions mainly includes the size and shape changes of the pore structure. Figure 16 illustrates the sandstone meso-pore development during the freeze-thaw cycles.

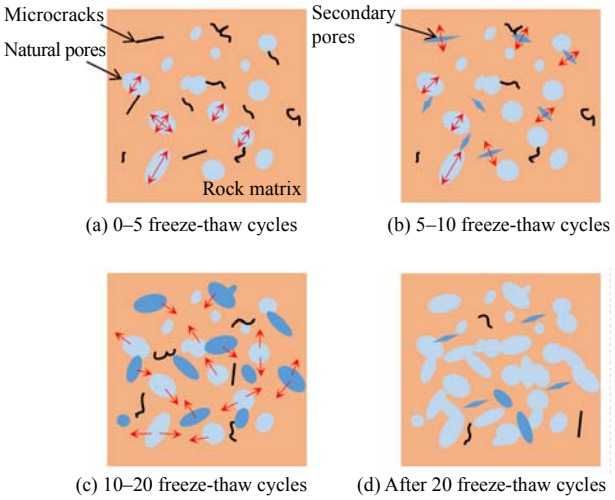

Fig.16 Evolution mechanism of the sandstone pores

In the stage with the freeze-thaw cycles of 0–5, the rock particles are still closely connected and the cohesion is high. The natural pores increase under the effect of water freeze-thaw and the corresponding expansion-shrinkage, and the porosity increases slightly. Negative pressure area appears inside the pores. Part of the free water migrates to the micro-cracks under the action of negative pressure, and the macroscopic strength and elastic modulus of the sandstone decrease. The frost-heave force generated by the condensation of pore water does not significantly damage the material structure. In the stage with the freeze-thaw cycles of 5–10, the pore water produces the "ice jam effect" under the repeated freezing and thawing. The natural pores grow further, and the migrating free water causes the further cracking of micropores and microcracks. This causes irreversible expansion of intergranular channels and development of secondary pores. At this moment, the porosity increases

dramatically, but the pore fractal dimension fails to change significantly.

During the 10^{th} to 20^{th} freeze-thaw cycles, the natural and secondary pores develop together under the uneven expansion of rock particles and the repeated phase change of water ice in defects, and the increase of porosity and the decrease of pore fractal dimension are both small at this stage. Considering the reason, we believe that the rock matrix has been squeezed by the frost-heave force generated by the freezing of the pore water, which enhances the cohesion and relieves the frost-heave effect to some extent. On the other hand, the hydrostatic pressure of pore water causes the neighbouring pores to squeeze each other, which limits the development of damage. Both of them limit the freeze-thaw effect to a certain extent. After 20 freeze-thaw cycles, the connection between rock particles has been greatly weakened. Stress concentration appears in the pore space where the spatial curvature and gradient change is abrupt. The pores have been further opened and fractured, and the original multi-dispersed and randomly distributed capillary pores expand and coalesce, and evolve into ultra-capillary pores. The originally complex spatial pattern forms relatively simple large pores and connected pores, which promote the extension and expansion of the original pores to form cracks, and to develop into macroscopic cracks. This results in a serious decrease of the rock strength and the elastic modulus[33–35]. The above discussion describes the evolution of the effects of mesostructural changes on the macroscopic properties of materials. It interprets the macroscopic mechanical behaviour of the frozen-thawed sandstone based on the physical nature of the meso-structure of the material.

6 Conclusion

(1) Based on the genetic optimization model using the maximum entropy of the image, we use a probabilistic method to comprehensively search for the overall entropy of the image, and quickly and accurately select the optimal threshold for binary image segmentation. The distribution of rocks and defects in the processed images is clear and intuitive, which provides the fundamentals for meso-feature extraction and damage characteristics research.

(2) The digital image matrix theory, the three-dimensional reconstruction and the box counting method can effectively extract the rock porosity and the pore fractal dimension, which can be used to characterize the pore size and the pore structural shape distribution inside the rock. With the increase of freeze-thaw cycles, the volume porosity increases obviously, but the pore fractal dimension decreases. On the mesoscopic scale, the pores expand and its number increases, but the structural complexity decreases.

(3) The macro- and meso-damage variables defined by the conventional methods show great differences in their evolution plots because there misses the consideration of the initial damage of the rock and the effect of the morphological changes of the meso-structure on the damage expansion. Based on the two physical mechanisms including pore size and pore structural morphology, we propose a new freeze-thaw meso-damage variable definition. It considers the natural damage of rocks to define the freeze-thaw macroscopic damage variable. It achieves the cross-scale damage identification of the same object, and provides a new quantitative method for multi-scale research on the damage characteristics of frozen-thawed red sandstone.

(4) By using the multi-scale study method to analyze the damage variation of frozen-thawed rocks, the meso-structural characteristics can be used to predict the macro-mechanical characteristics. This quantitatively describes the relationship between the mesoscopic structural variation and the macroscopic mechanical response during those freeze-thaw cycles. It can analyze the dominant roles of pore size and pore structural or morphological changes in the damage of frozen-thawed rocks. It explains the macroscopic sandstone freeze-thaw mechanical failure by using the meso-structural physical mechanisms.

References

[1] YANG Geng-she, SHEN Yan-jun, JIA Hai-liang, et al. Research progress and tendency in characteristics of multi-scale damage mechanics of rock under freezing-thawing[J]. Chinese Journal of Rock Mechanics and Engineering, 2018, 37(3): 545–563.

[2] XU Guang-miao, LIU Quan-sheng. Analysis of mechanism of rock failure due to freeze-thaw cycling and mechanical testing study on frozen-thawed rocks[J]. Chinese Journal of Rock Mechanics and Engineering, 2005, 24(17): 3076–3082.

[3] YANG Geng-she, XIE Ding-yi, ZHANG Chang-qing, et al. CT indentification of rock damage properties[J]. Chinese Journal of Rock Mechanics and Engineering, 1996, 15(1): 48–54.

[4] APPOLONI C R, FERNANDES C P, RODRIGUES C. X-ray microtomography study of a sandstone reservoir rock[J]. Nuclear Instruments and Methods in Physics Research A: Accelerators, Spectrometers, Detectors and Associated Equipment, 2007, 580(1): 629–632.

[5] ZHU Hong-guang, XIE He-ping, YI Cheng, et al. CT identification of microcracks evolution for rock materials[J]. Chinese Journal of Rock Mechanics and Engineering, 2011, 30(6): 1230–1238.

[6] MA Tian-shou, CHEN Ping. Study of meso-damage characteristics of shale hydration based on CT scanning technology[J]. Petroleum Exploration and Development, 2014, 41(2): 227–233.

[7] HAN N, TIAN W. Experimental study on the dynamic mechanical properties of concrete under freeze-thaw cycles[J]. Structural Concrete, 2018, 19(5): 1353–1362.

[8] LIU Hui, YANG Geng-she, YE Wan-jun, et al. Analysis of water and ice content and damage characteristics of the frozen rock during freezing based on the three-valued segmentation of CT images[J]. Journal of Mining and

Safety Engineering, 2016, 33(6):1130–1137.

[9] ZHANG Hui-mei, WANG Huan, ZHANG Jia-fan, et al. Analysis of meso-damage characteristics of freeze-thaw rock on CT scale[J]. Journal of Liaoning Technical University: Natural Science, 2020, 39(1): 51–56.

[10] CHIARAMONTI A N, GOGUEN J D, GARBOCZI E J. Quantifying the 3-Dimensional shape of lunar regolith particles using X-ray computed tomography and scanning electron microscopy at sub-γ resolution[J]. Microscopy & Microanalysis, 2017, 23(Suppl.1): 2194–2795.

[11] PENG Rui-dong, YANG Yan-cong, JU Yang, et al. Computation of fractal dimension of rock pores based on gray CT images[J]. Chinese Science Bulletin, 2011, 56(26): 2256–2266.

[12] LI Shou-ju, LI De, WU Li, et al. Meso-simulation and fractal characteristics for uniaxial compression test of inhomogeneous rock[J]. Journal of China Coal Society, 2014, 39(5): 849–854.

[13] PARK J, HYUN C U, PARK H D. Changes in microstructure and physical properties of rocks caused by artificial freeze-thaw action[J]. Bulletin of Engineering Geology and the Environment, 2015, 74(2): 555–565.

[14] DE KOCK T, BOONE M A, DE SCHRYVER T, et al. A pore-scale study of fracture dynamics in rock using X-ray micro-CT under ambient freeze-thaw cycling[J]. Environmental Science and Technology, 2015, 49(5): 2867–2874.

[15] CHEN J, DENG X, LUO Y, et al. Investigation of microstructural damage in shotcrete under a freeze–thaw environment[J]. Construction & Building Materials, 2015, 83: 275–282.

[16] LIU Xiang-jun, XIONG Jian, LIANG Li-xi, et al. Study on the charac-teristics of pore structure of tight sand based on micro-CT scanningand itsinfluence on fluid flow[J]. Progress in Geophysics, 2017, 32(3): 1019–1028.

[17] SONG Yong-jun, YANG Hui-min, ZHANG Lei-tao, et al. CT real-time monitoring on uniaxial damage of frozen red sandstone[J]. Rock and Soil Mechanics, 2019, 40(Suppl.1): 152–160.

[18] LANG Ying-xian, LIANG Zheng-zhao, DUAN Dong, et al. Three-dimensional parallel numerical simulation of porous rocks based on CT technology and digital image processing[J]. Rock and Soil Mechanics, 2019, 40(3): 1204–1212.

[19] YU Cheng-bo. Digital image processing and MATLAB implementation[M]. Chongqing: Chongqing University Press, 2003.

[20] ZHANG Jia-fan, ZHANG Xue-jiao, YANG Geng-she, et al. A method of rock CT image segmentation and quantification based on clustering algorithm[J]. Journal of Xi'an University of Science and Technology, 2016, 36(2): 171–175.

[21] WU Ling-yan, SHEN Ting-zhi, FANG Zi-wen. An Image segmentation method using the entropy of histogram and genetic algorithms[J]. Acta Armamentarh, 1999, 20(3): 255–258.

[22] MA Shao-peng, LIU Shan-jun, ZHAO Yong-hong. Gray correlation of digital images from loaded rock specimen surface to evaluate its damage evolution[J]. Chinese Journal of Rock Mechanics and Engineering, 2006, 25(3): 590–595.

[23] XIE He-ping, XUE Xiu-qian. Mathematical basis and methods in fractal application[M]. Beijing: Science Press, 1998.

[24] ZOU Fei, LI Hai-bo, ZHOU Qing-chun, et al. Fractal features study of rock-like material damage based on gray correlation of digital images[J]. Rock and Soil Mechanics, 2012, 33(3): 731–738.

[25] ZHANG Shu-juan, LAI Yuan-ming, SUN Zhi-zhong, et al. State-of-art and development in meso-damage of rock experiment by the use of X-ray computed tomography[J]. Journal of Gansu Sciences, 2004, 16(1): 96-100.

[26] LIU Quan-sheng, HUANG Shi-bing, KANG Yong-shui, et al. Fatigue damage model and evaluation index for rock mass under freezing-thawing cycles[J]. Chinese Journal of Rock Mechanics and Engineering, 2015, 34(6): 1116–1127.

[27] JIA Hai-liang, LIU Qing-bing, XIANG Wei, et al. Damage evolution modelof saturated sandstone under freeze-thaw cycles[J]. Chinese Journal of Rock Mechanics and Engineering, 2013, 32(Supp.2): 3049–3055.

[28] LAI Yong, ZHANG Yong-xing. Study on macro- and meso-damage composite model of rock and crack propagation rule[J]. Chinese Journal of Rock Mechanics and Engineering, 2008, 27(3): 535–542.

[29] ZHAO Tao, YANG Geng-she, XI Jia-mi, et al. Experimental study of the macro and micro-scopic damage of Cretaceous sandstone subjected to freeze-thaw cycles[J]. Journal of Xi'an University of Science and Technology, 2019, 39(2): 241–248.

[30] SONG Zhao-yang. Study on meso-structure characteristics and deformation and failure mechanism of weakly cemented coarse-grained sandstone and its application[J]. Chinese Journal of Rock Mechanics and Engineering, 2018, 37(3): 779.

[31] WANG J, YAN H. DEM analysis of energy dissipation in crushable soils[J]. Soils and Foundations, 2012, 52(4): 644–657.

[32] WANG Li, LI Xi-an, ZHAO Ning, et al. Effect of clay content on physical and mechanical properties of loess soils[J]. The Chinese Journal of Geological Hazard and Control, 2018, 29(3): 133-143.

[33] SHEN Yan-jun, YANG Geng-she, WANG Ting, et al. Evaluation of frost heave force models of pore/fissure in rock and their applicability[J]. Journal of Glaciology and Geocryology, 2019, 41(1): 117–128.

[34] GONG Wei-li, LI Chen. Multi-scale and anisotropic characterization of coal structure based on SEM image analysis[J]. Chinese Journal of Rock Mechanics and Engineering, 2010, 29(4): 2681–2689.

[35] CONG Hai-long, WU Zi-sen, LI Hong, et al. Pore-scale stress sensi-tivity analysis of tight sandstone[J]. Science Technology and Engineering, 2019, 19(15): 105–110.